

# Signatures of a gap in the conductivity of graphene

Joaquín E. Drut<sup>1</sup>, Timo A. Lähde<sup>2</sup> and Eero Tölö<sup>2</sup>

<sup>1</sup>*Department of Physics, The Ohio State University, Columbus, OH 43210-1117, USA and*

<sup>2</sup>*Helsinki Institute of Physics and Department of Applied Physics, Aalto University, FI-02150 Espoo, Finland*

(Dated: September 12, 2018)

The electrical conductivity of suspended graphene has recently been measured for the first time, and found to behave as  $\sigma \sim \sqrt{|n|}$  as expected for Dirac quasiparticles at large carrier density. The charge inhomogeneity is strongly reduced in suspended samples, which revealed an unexpected insulating trend in  $\sigma(T)$ . Above a transitional density  $n^*$ , the temperature dependence was found to revert to metallic. We show that these features of the DC conductivity are consistent with a simple model of gapped Dirac quasiparticles, with specific signatures of a gap in the vicinity of the charge-neutrality point. Our findings are reminiscent of the conductivity profile in semiconducting materials, exhibiting a thermal activation for  $T \geq \tilde{T}$  and a weakly  $T$ -dependent background for  $T \leq \tilde{T}$ , where  $\tilde{T}$  is given by the saturation density  $\tilde{n}$  associated with the residual charge inhomogeneity. We discuss possible origins of a bandgap in graphene as well as alternative scenarios.

PACS numbers: 73.63.Bd, 71.30.+h, 05.10.Ln

The experimental study of graphene has recently progressed towards an improved understanding of the intrinsic properties of this new carbon nanomaterial. Notably, a clear signal for the fractional quantum Hall effect has been found [1, 2], and carrier mobilities far in excess of silicon-based devices have been reached [3]. While the high quality of graphene and the Dirac nature of the charge carriers is by now well established, the issue of gap formation has remained far less clear. Indeed, several features suggestive of a gap but difficult to interpret have been reported under various circumstances. The Lanzara group has performed ARPES studies [4, 5] of graphene layers on a substrate, whereby a gap-like feature was detected and attributed to substrate effects. On the other hand, the conductivity of suspended graphene devices was characterized by the Kim group [6] and the Andrei group [7]. In addition to demonstrating a strongly  $T$ -dependent DC conductivity  $\sigma$ , a transitional carrier density  $n^*$  was found, where  $\sigma(T)$  changes from metallic to insulating. A different perspective is provided by the Andrei group in Ref. [8] via STM spectroscopy of decoupled graphene flakes on graphite, where a  $\sim 10$  meV gap centered on the Dirac point was found at zero magnetic field, accompanied by a corresponding splitting of the lowest Landau level.

On the theoretical side, a quantitative explanation of  $\sigma(n, T)$  has remained elusive. For instance, the appearance of a transitional density  $n^*$  is incompatible with electron-phonon scattering [6, 9], while electron-electron scattering leads to metallic behavior at the neutral point [10]. A qualitative description of the empirical  $\sigma(n, T)$  is given by Landauer transport theory for ballistic graphene [11]. The Hall probe lead geometry of Ref. [6] minimizes the effects of a finite sample size, whereas the two-lead geometry of Ref. [7] is better described in the Landauer approach. Our primary objectives are to determine whether the measured  $\sigma(T)$  of Ref. [6] at the neutral point can be quantitatively described in terms of free

gapped Dirac quasiparticles and a weakly  $T$ -dependent background, and whether such a description is consistent with  $\sigma(n, T)$  at finite carrier density.

The rationale for the gapped quasiparticle scenario is as follows: Initially, the suspended samples of Ref. [6] showed an essentially  $T$ -independent DC conductivity, which upon current-annealing acquired a pronounced  $T$ -dependence of insulating type. While the increase in resistivity at low  $T$  remained modest (a factor of  $\sim 3$  in the range 5 – 150 K), the data suggests the existence of two regimes, reminiscent of conventional semiconductors [12]: a low- $T$  regime (5 – 35 K) where  $\sigma$  is dominated by a weakly  $T$ -dependent background  $\sigma_{bg}$ , and a thermally activated regime (35 – 150 K) where  $\sigma$  increases rapidly with  $T$ . Notably, several mechanisms for gap generation have been proposed, such as explicit breaking of the sublattice symmetry by mechanical strain [13], or spontaneous induction of a Mott insulating state via strong Coulomb interactions [14]. It is plausible that  $\sigma_{bg}$  is due to residual charge density inhomogeneities [15] which, however, are reduced by an order of magnitude compared with samples on a substrate [7]. Regardless of the origin of  $\sigma_{bg}$ , we find that it can be reliably subtracted.

The Hamiltonian describing Dirac quasiparticles with a gap  $\Delta$  and Fermi velocity  $v_F \simeq c/300$  is given by

$$H = \sigma_1 v_F k_1 + \sigma_2 v_F k_2 + \sigma_3 \Delta/2, \quad (1)$$

where the  $\sigma_i$  are Pauli matrices, and we account for the spin and valley degeneracy below. From this starting point,  $\sigma$  is calculated as the diagonal part of the conductivity tensor  $\sigma_{\mu\nu}$ , given by the Kubo formula

$$\sigma_{\mu\mu} = \frac{\pi e^2}{\hbar} \int_{-\infty}^{\infty} d\epsilon \text{Tr} \left\{ [H, r_\mu] \delta \left( H - \epsilon - \frac{\omega}{2} \right) [H, r_\mu] \right. \\ \left. \times \delta \left( H - \epsilon + \frac{\omega}{2} \right) \right\} \frac{f(\beta\epsilon + \frac{\beta\omega}{2}) - f(\beta\epsilon - \frac{\beta\omega}{2})}{\omega}, \quad (2)$$

where  $\beta \equiv 1/k_B T$  and the Fermi function is given by

$f(x) = 1/(1 + \exp(x))$ . The contribution  $\sigma_q$  of the Dirac quasiparticles to the conductivity of a graphene mono-layer is then

$$\sigma_q = \frac{4e^2 \pi}{h} \frac{1}{2} \int_{-\infty}^{\infty} d\epsilon \int_{\Delta/2}^{\infty} d\xi \xi \mathcal{T}_\omega(\xi, \epsilon) \times \frac{f(\beta\epsilon - \frac{\beta\omega}{2} - \beta\mu) - f(\beta\epsilon + \frac{\beta\omega}{2} - \beta\mu)}{\omega}, \quad (3)$$

where  $\mu$  is the chemical potential, and the factor of 4 accounts for the spin and valley degrees of freedom. We find

$$\begin{aligned} \mathcal{T}_\omega(\xi, \epsilon) \equiv & \frac{\xi^2 + \Delta^2/4}{\xi^2} \left[ \delta_\eta \left( \xi + \epsilon + \frac{\omega}{2} \right) \delta_\eta \left( \xi - \epsilon + \frac{\omega}{2} \right) \right. \\ & \left. + \delta_\eta \left( \xi + \epsilon - \frac{\omega}{2} \right) \delta_\eta \left( \xi - \epsilon - \frac{\omega}{2} \right) \right] \\ & + \frac{\xi^2 - \Delta^2/4}{\xi^2} \left[ \delta_\eta \left( \xi - \epsilon - \frac{\omega}{2} \right) \delta_\eta \left( \xi - \epsilon + \frac{\omega}{2} \right) \right. \\ & \left. + \delta_\eta \left( \xi + \epsilon + \frac{\omega}{2} \right) \delta_\eta \left( \xi + \epsilon - \frac{\omega}{2} \right) \right], \quad (4) \end{aligned}$$

where  $\eta$  is the scattering rate of the quasiparticles, which can be accounted for [16] by broadening the delta functions according to  $\pi\delta_\eta(x) \equiv \eta/(x^2 + \eta^2)$ . While the  $T$ -dependence of  $\eta$  is *a priori* unknown, we find that the scenario of constant  $\beta\eta$ , which may be ascribed to scattering off impurities or thermally generated ripples [16], is strongly favored by the available data in the range  $35 \text{ K} \leq T \leq 150 \text{ K}$ . The integral over  $\xi$  in Eq. (3) can be performed analytically, and in the DC limit it yields

$$\int_{\Delta/2}^{\infty} d\xi \xi \mathcal{T}_0(\xi, \epsilon) = \frac{1}{2\pi} - \frac{\Delta^2 - 4|z|^2}{16\pi\epsilon\eta} \arg(\Delta^2 - 4z^2), \quad (5)$$

where  $z = \epsilon + i\eta$ . The dependence of  $\sigma_q$  on  $\beta\Delta$  and  $\beta\eta$  is illustrated in Fig. 1.

We now analyze the data of Ref. [6] on the suspended graphene devices S1, S2 and S3 in terms of the expression  $\sigma \equiv \sigma_q + \sigma_{bg}$ , where  $\sigma_{bg}$  denotes the background conductivity. The simplest form compatible with the low- $T$  data is the linear one  $\sigma_{bg} \equiv \sigma_0(1 - T_0/T)$ . A more specific choice is the Variable-Range Hopping (VRH) law  $\sigma_{bg} \equiv \sigma_0 \exp[-(T_0/T)^\alpha]$  encountered in conventional semiconductors [12]. While the former can be viewed as a linearized VRH expression, it cannot remain valid at arbitrarily low  $T$  as it becomes unphysical in that limit. As the  $T$ -dependence of the background is experimentally found to be weak, the choice of linear versus VRH description has very little impact on the analysis.

In order to determine  $\sigma_{bg}$  in an unbiased fashion, we first fix  $\sigma_0$  and  $T_0$  using the data in the low- $T$  region where thermal activation is negligible. The next step is to subtract  $\sigma_{bg}$  at all  $T$ , and determine  $\beta\eta$  and  $\Delta$  by fitting  $\sigma_q$  to the resulting dataset. Finally, the results were confirmed by a simultaneous fit of all four parameters to the full dataset. In all cases negligible variation was

observed, indicating that  $\sigma_0$  and  $T_0$  are effectively uncorrelated with  $\beta\eta$  and  $\Delta$ . The optimal parameter values are summarized in Table I, and the results are plotted against the data of Ref. [6] in Fig. 2.

Our findings indicate that the suspended graphene devices of Ref. [6] exhibit, upon subtraction of  $\sigma_{bg}$ , a thermally activated component which can be well described in terms of Eq. (3) from  $T \sim 150 \text{ K}$  down to  $T \sim 35 \text{ K}$ , where the signal is lost due to limited measurement accuracy. As shown in Fig. 2, this corresponds to exponential behavior over more than two orders of magnitude, with bandgaps in the range  $\sim 25 - 40 \text{ meV}$ . The value  $\beta\eta \simeq 0.1$  obtained for samples S1 and S2 is consistent with the high carrier mobilities and long mean free paths reported in Ref. [6]. Specifically, for  $T = 35 - 150 \text{ K}$  we find  $\eta = 3.5 - 15 \text{ K}$ , with corresponding mean free paths of  $\hbar v_F/\eta \sim 2.0 - 0.5 \mu\text{m}$ . For such low values of  $\beta\eta$ , the rate of exponential decay is characterized by  $\Delta$  whereas  $\beta\eta$  mainly determines the amplitude. It is noteworthy that the values of  $\beta\eta$  and  $\Delta$  are roughly sample-independent. We have checked that fits with zero gap ( $\Delta = 0$ ), constant  $\eta$  or zero background are incompatible with the data. Above  $T \sim 150 \text{ K}$ , the data deviate from a description with constant  $\beta\eta$ , which may be ascribed to increasing phonon scattering at high  $T$  [6].

Once the description of the zero-density data is fixed, it is possible to predict  $\sigma$  at *finite* carrier density  $n$ , with

$$n \equiv \frac{2}{\pi(\hbar v_F \beta)^2} \int_0^\infty dx x \times [g_+(x, \beta\Delta, \beta\mu) - g_-(x, \beta\Delta, \beta\mu)], \quad (6)$$

where  $g_\pm(x, \beta\Delta, \beta\mu) \equiv f(\sqrt{x^2 + (\beta\Delta/2)^2} \mp \beta\mu)$ . It should be emphasized that  $\sigma(n)$  is strongly dependent

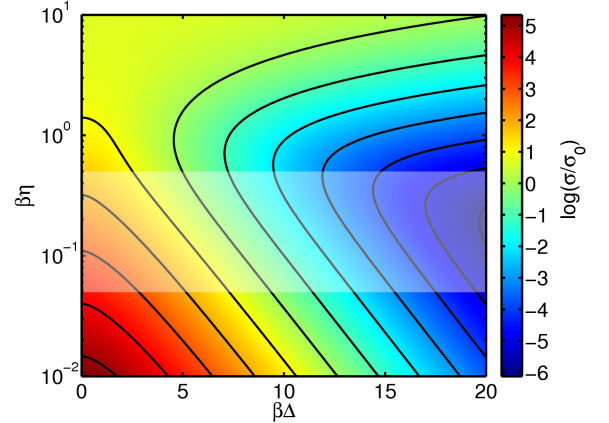


FIG. 1: (Color online) DC conductivity  $\sigma_q$  as a function of  $\beta\Delta$  and  $\beta\eta$ , shown semilogarithmically. For  $\beta\Delta \gg 1$ ,  $\sigma_q$  decreases exponentially when  $\beta\eta \ll 1$ , while for  $\beta\eta \gg 1$  any signature of a gap is washed out by the large scattering rate. For  $\beta\eta \ll 1$ ,  $\sigma_q$  decreases with  $\beta\eta$ , while for  $\beta\eta \gg 1$  this behavior is reversed. The shaded area denotes the approximate range in  $\beta\eta$  for suspended graphene samples.

TABLE I: Optimal parameter values for the suspended graphene devices of Ref. [6], corresponding to the analysis in Fig. 2. Similar results for the gap  $\Delta$  and the scattering rate  $\beta\eta$  were obtained by subtracting the background conductivity using a linear form or a VRH description with  $\alpha \sim 1/3$ . Entries labeled by an asterisk (\*) indicate that  $\beta\eta$  cannot be constrained due to lack of information on the normalization factor  $\sigma(5\text{K})$ , which is not known for device S3. The resulting uncertainty in  $\Delta$  is negligible.

sample	$\beta\eta$	$\Delta[\text{meV}]$	$\sigma_0[\text{k}\Omega^{-1}]$	$T_0$ [K]	$\chi^2/N_{\text{dof}}$
S1( $\alpha=1/3$ )	0.103(3)	36.8(1)	0.530(6)	0.027(7)	1.6
S2( $\alpha=1/3$ )	0.105(1)	26.2(1)	0.485(5)	0.85(6)	1.1
S3( $\alpha=1/3$ )	0.070(1)*	35.8(1)	0.471(2)	1.87(8)	4.1
S3( $\alpha=1/4$ )	0.070(1)*	36.4(1)	0.551(2)	2.81(8)	4.0
S3(linear)	0.070(1)*	32.0(1)	0.339(1)	2.21(1)	7.1

on  $\beta\eta$ , which is obtained via analysis of the quasiparticle contribution to  $\sigma(T)$  at  $n = 0$ . In Fig. 3, we show that the data of Ref. [6] at finite  $n$  is well described using the parameters of Table I, as obtained from the gapped quasiparticle analysis at  $n = 0$ . Notice also that the experimentally observed  $\sigma \sim \sqrt{|n|}$  dependence is reproduced (see Fig. 3, inset), as well as the transitional carrier density  $n^* \sim 10^{10} \text{ cm}^{-2}$  which was identified in Ref. [6] as separating metallic ( $|n| > n^*$ ) and insulating ( $|n| < n^*$ ) regimes in  $\sigma(n, T)$ . In the metallic regime, we recover the experimentally observed resistivity  $\rho \sim T$ .

While a gap in the quasiparticle spectrum is an attractive interpretation of the thermally excited conductivity, it should be noted that a number of other mechanisms can yield similar results. These include localized disorder [18], scattering by screened charged impurities [19], and transport gaps due to quantum confinement [11]. Nevertheless, the gapped scenario is appealing as it provides a straightforward and consistent description of the  $T$ - and  $n$ -dependence of  $\sigma$ , involving only quasiparticle excitations and an inhomogeneous regime close to the Dirac point. A plausible mechanism for gap generation in suspended graphene is given by the excitonic scenario, where a gap is dynamically generated by strong electron-electron interactions [20, 21]. This idea has recently been revived based on Lattice Monte Carlo simulations of the low-energy effective field theory of graphene [22, 23]. It is noteworthy that graphene flakes decoupled from underlying graphite layers have been found to exhibit a  $\sim 10 \text{ meV}$  bandgap at zero magnetic field, with a corresponding splitting of the lowest Landau level of similar magnitude [8].

What is the origin of the observed background conductivity? Empirically, the physics at the Dirac point is obscured by charge density inhomogeneities [6, 7], also referred to as “puddles”, where  $n$  saturates to a finite value. The scale at which this happens for presently available samples is  $\tilde{n} \sim 10^{11} \text{ cm}^{-2}$  in non-suspended graphene,

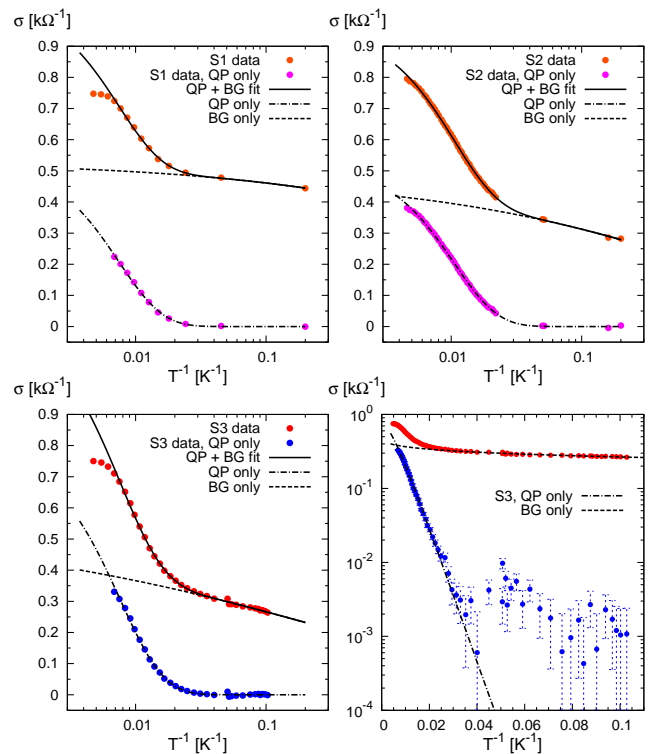


FIG. 2: (Color online) Dirac Quasiparticle (QP) and background (BG) components (see Table I) of the DC conductivity for the suspended graphene devices S1–S3, reproduced from Ref. [6]. All devices show a “knee” separating the thermally activated and background regions. After background subtraction, device S3 exhibits exponential behavior over more than two orders of magnitude. The slight curvature at high  $T$  is due to the finite scattering rate  $\beta\eta$ .

and  $\tilde{n} \sim 10^9 \text{ cm}^{-2}$  in suspended graphene [6, 7]. One can define energy and temperature scales  $\tilde{E}$  and  $\tilde{T}$  via

$$\tilde{E} \equiv k_B \tilde{T} \simeq \hbar v_F \sqrt{\pi \tilde{n}}, \quad (7)$$

below which the description in terms of Dirac cones breaks down. Typically,  $\tilde{E} \sim 40 \text{ meV}$  in graphene on a substrate, while in suspended samples  $\tilde{E} < 10 \text{ meV}$  as  $\tilde{n}$  is reduced by an order of magnitude, thereby making it possible to access the physics at the Dirac point. Thus a bandgap of  $\Delta \sim 30 \text{ meV}$  is likely to be obscured by charge inhomogeneities in the non-suspended samples, whereas in suspended ones such a gap should be (partially) accessible. In samples with yet lower inhomogeneity, one should observe a decrease in the low- $T$  background conductivity and an enhancement of the strongly  $T$ -dependent quasiparticle contribution. A description of  $\sigma_{bg}$  which is compatible with data is given by the VRH model [12], which describes the residual conductivity in semiconducting materials when thermal excitation is negligible. If the background conductivity is indeed of the VRH form with  $\alpha = 1/3$  (as expected in 2D systems), it may indicate hopping between localized states. How-

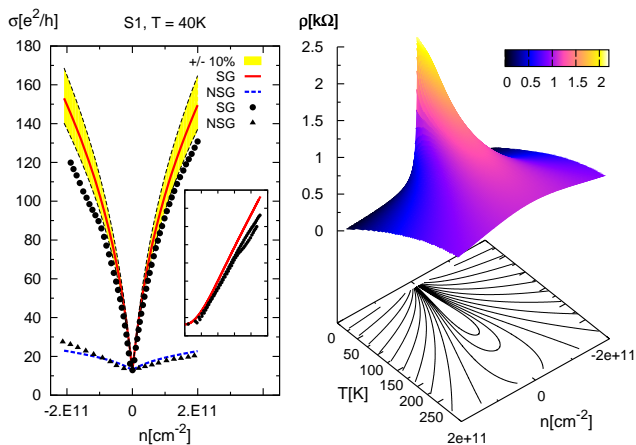


FIG. 3: (Color online) Left panel: Carrier density dependence of the DC conductivity  $\sigma \equiv \sigma_q + \sigma_{bg}$  for the suspended graphene device S1 at  $T = 40$  K for our model (solid red line) and experiment [6] before (triangles) and after (circles) current-annealing. The dashed blue line corresponds to  $\beta\eta \sim 1.4$ , although the properties before annealing are likely dominated by charged impurities [6]. Inset:  $\sigma$  as a function of  $\sqrt{|n|}$ . Right panel: Resistivity  $\rho(n, T)$  for device S1. As in Ref. [6],  $\partial\rho/\partial T$  is metallic above  $n^* \sim 10^{10} \text{ cm}^{-2}$ .

ever, the data are inconclusive as the variation of  $\sigma$  is very mild at low  $T$ .

In summary, we have explored the signatures of a bandgap in the DC conductivity of graphene and showed that the empirical conductivity profiles  $\sigma(n, T)$  are consistent with an interpretation in terms of Dirac quasiparticles with a non-zero bandgap  $\Delta$ . However, the associated thermally activated behavior is partially obscured below an empirically observed characteristic scale  $\tilde{n}$ , where the carrier density as a function of the gate voltage saturates. As gapped graphene is of great interest for nanoelectronic applications, a fully non-perturbative calculation (such as Lattice Monte Carlo) of the transport properties, including the effects of strong electron-electron interactions, is clearly called for. Such calculations also appear timely, as recent experimental work [1, 2, 24] at finite magnetic field has demonstrated a rich spectrum of phenomena closely related to Dirac physics at strong Coulomb coupling.

We acknowledge support under U.S. DOE Grants No. DE-FG02-00ER41132 and DE-AC02-05CH11231, UNEDF SciDAC Collaboration Grant No. DE-FC02-07ER41457 and NSF Grant No. PHY-0653312. This study was supported in part by the Academy of Finland through its Centers of Excellence Program (2006 - 2011), the Vilho, Yrjö, and Kalle Väisälä Foundation of the Finnish Academy of Science and Letters, and by an allocation of computing time from the Ohio Supercomputer Center. We thank A. H. Castro Neto, R. J. Furnstahl, M. Randeria, K. I. Bolotin, E. Y. Andrei, and P. Hako-

nen for instructive discussions and comments. Part of this work used the CUBPACK numerical quadrature routine.

- [1] X. Du *et al.*, Nature **462**, 192 (2009); D. A. Abanin *et al.*, Phys. Rev. B **81**, 115410 (2010).
- [2] K. I. Bolotin *et al.*, Nature **462**, 196 (2009);
- [3] K. I. Bolotin *et al.*, Solid State Commun. **146**, 351 (2008).
- [4] S. Y. Zhou *et al.*, Nature Mat. **6**, 770 (2007); A. Bostwick *et al.*, Nature Phys. **3**, 36 (2007).
- [5] S. Y. Zhou *et al.*, Physica E **40**, 2642 (2008); Nature Mat. **7**, 259 (2008).
- [6] K. I. Bolotin *et al.*, Phys. Rev. Lett. **101**, 096802 (2008); V. Crespi, Physics **1**, 15 (2008).
- [7] X. Du *et al.*, Nature Nanotechnology **3**, 491 (2008).
- [8] G. Li, A. Luican, E. Andrei, Phys. Rev. Lett. **102**, 176804 (2009).
- [9] E. H. Hwang, S. Das Sarma, Phys. Rev. B **77**, 115449 (2008); F. T. Vasko, V. Ryzhii, *ibid.* B **76**, 233404 (2007); T. Stauber, N. M. R. Peres, F. Guinea, *ibid.* B **76**, 205423 (2007).
- [10] M. Müller, L. Fritz, S. Sachdev, Phys. Rev. B **78**, 115406 (2008); L. Fritz *et al.*, *ibid.* B **78**, 085416 (2008).
- [11] J. Tworzydło *et al.*, Phys. Rev. Lett. **96**, 246802 (2006); M. Müller, M. Bräuninger, B. Trauzettel, *ibid.* **103**, 196801 (2009).
- [12] N. F. Mott, *Metal-Insulator Transitions*, 2<sup>nd</sup> ed. (Taylor & Francis, London, 1990).
- [13] T. Yu *et al.*, J. Phys. Chem. C **112** (33), 12602 (2008); Z. H. Ni *et al.*, ACS Nano **3** (2), 483 (2009); V. M. Pereira, A. H. Castro Neto, Phys. Rev. Lett. **103**, 046801 (2009); V. M. Pereira, A. H. Castro Neto, N. M. R. Peres, Phys. Rev. B **80**, 045401 (2009).
- [14] A. H. Castro Neto, Physics **2**, 30 (2009).
- [15] Y. Zhang *et al.*, Nature Phys. **5**, 722 (2009).
- [16] K. Ziegler, Phys. Rev. Lett. **97**, 266802 (2006); Phys. Rev. B **75**, 233407 (2007).
- [17] Y.-W. Son, M. L. Cohen, S. G. Louie, Phys. Rev. Lett. **97**, 216803 (2006); L. Yang *et al.*, *ibid.* **99**, 186801 (2007); B. Sahu *et al.*, Phys. Rev. B **78**, 045404 (2008).
- [18] N. M. R. Peres, F. Guinea, A. H. Castro Neto, Phys. Rev. B **73**, 125411 (2006).
- [19] E. H. Hwang, S. Das Sarma, Phys. Rev. B **79**, 165404 (2009).
- [20] P. I. Fomin *et al.*, Nucl. Phys. B **110**, 445 (1976); Riv. Nuovo Cimento, **6** 1 (1983); V. A. Miransky, *ibid.* **90** A 149 (1985).
- [21] D. V. Khveshchenko, Phys. Rev. Lett. **87**, 246802 (2001); J. Phys.: Condens. Matter **21**, 075303 (2009); D. V. Khveshchenko, H. Leal, Nucl. Phys. B **687**, 323 (2004).
- [22] J. E. Drut, T. A. Lähde, Phys. Rev. Lett. **102**, 026802 (2009); Phys. Rev. B **79**, 165425 (2009); *ibid.* **79**, 241405(R) (2009).
- [23] S. J. Hands, C. G. Strouthos, Phys. Rev. B **78**, 165423 (2008); W. Armour, S. J. Hands, C. G. Strouthos, *ibid.* **81**, 125105 (2010); [arXiv:0908.0118].
- [24] J. Checkelsky, L. Li, N. P. Ong, Phys. Rev. B **79**, 115434 (2009).